Int J Mater Form (2016) 9:85–100
DOI 10.1007/s12289-014-1210-y

ORIGINAL RESEARCH

Parameter identification and computational simulation of polyurethane foaming process by finite pointset method

Hichem Abdessalam · Boussad Abbès · Yuming Li · Ying-Qiao Guo · Elvis Kwassi · Jean-Luc Romain

Received: 15 August 2014 / Accepted: 16 December 2014 / Published online: 16 January 2015

Abstract Numerical simulation of the polyurethane foaming process is a valuable method to analyze the molding process at an early stage of product development to shorten time-to-market cycles and cut costs by using fewer prototypes. However, this process involves highly coupled thermo-chemo-rheological modeling and needs adequate model parameters' identification. A theoretical model including chemical reactions and thermo-rheological coupling of conservation equations was developed. Based on the theoretical model, three-dimensional numerical simulation for mold filling of the polyurethane foam was carried out by using Finite Pointset Method (FPM) to predict flow field, flow front advancement, temperature and density distributions during mold filling. A FOAMAT system was used to monitor foam height rise and reaction temperature on a cylindrical test tube and foam viscosity was measured by using a dynamic rotational rheometer with parallel-plate system. The parameters of the model were identified by an inverse analysis method which consists in determining the parameters by comparing the computed quantities to those measured experimentally. The overall modeling was validated by using short shot foams obtained with a panel mold cavity. Mold filling of an automotive underlay carpet cavity was investigated numerically. Flow front results were successfully compared to short shot foams obtained with the industrial mold cavity.

Keywords Polyurethane foaming · Mold filling · Parameter identification · Finite Poinset Method

H. Abdessalam · B. Abbès (✉) · Y. Li · Y.-Q. Guo
GRESPI/MPSE, University of Reims Champagne-Ardenne, Campus du Moulin de la House, BP 1039, 51687 Reims Cedex 2, France
e-mail: boussad.abbes@univ-reims.fr

H. Abdessalam · E. Kwassi · J.-L. Romain
FAURECIA, Route de Villemontry, 08210 Mouzon, France

Introduction

Polyurethane foams are widely used in several applications such as automotive, aeronautic and buildings. These thermosetting materials offer many opportunities thanks to their wide range of stiffness, hardness and densities. After injection of the mixture of polyols, isocyanate, blowing agents, catalysts and other additives, the foam expansion starts in few seconds and fills out the mold cavity. During this process a number of defects (air entrapment, weld lines, unfilled regions in the mold…) may occur and can affect the quality of the final product. Thus, the modeling and the numerical simulation of the foaming process is very important during the mold design process to define suitable injection points and air vents to avoid the potential defects. By the simulation of foaming process, one can reduce the development delay and the costs by reducing the number of mold prototypes and the time for parameter settings of the process.

The modeling of the foaming process has been extensively studied and several models have been proposed to describe the foaming process at a microscopic scale [1–6] or macroscopic scale [7–9]. In the microscopic approach, a single [1, 2] or a multiple gas bubbles [3] in a polymeric melt are considered for the modeling of the polyurethane foaming. Amon and Denson [4] and Arefmanesh et al. [5, 6] used a microscopic cell model to predict macroscopic parameters of the foaming process such as the front evolution and the density decrease. For the macroscopic approach, the foam is supposed to be a pseudo-homogeneous phase whose expansion is governed by the evolution of its density either through an empirical equation [10] or by considering the contribution of the chemical reactions, the temperature and the viscosity evolution [11–14]. Baser and Khakhar [15] studied the foaming process for a polyurethane with a physical blowing agent considered as a pseudo-homogeneous phase. They have proposed two theoretical models by considering the foaming process controlled

only by heat generation or by heat generation and mass transfer. These models were used to predict the evolution in time of the temperature and the density of the foam. To identify the needed parameters for the *n*th order kinetic model used for the gelling reaction, they have used the temperature rise measurement for an adiabatic reaction of a non foaming mixture. Baser and Khakhar [11] have also studied the foaming process for polyurethane with a physical and chemical (water) blowing agents. They have supposed that the generation of the carbon dioxide gas is controlled by the rate of the reaction of isocyanate with water which was supposed to follow a first order kinetic model. The two reactions were assumed to be independent and their kinetic parameters have been identified separately. The parameters of the gelling reaction have been calculated using the same method as for the previous work [15]. For the blowing reaction, they monitored the foaming process with only chemical blowing agent. The rate of volume change was used to determine the parameters of the kinetic model.

One and two dimensional mathematical models based on the finite element method have been proposed by Lefebvre and Keunings [16, 17] to simulate the foaming process. By assuming the foam as a homogeneous compressible inelastic fluid, these models have been used to predict the evolution in time of macroscopic properties such as the density of the foam. The foaming was controlled by the decrease of the density which was supposed to be temperature-dependant and modeled by a mixture law of reactant and products densities. The evolution of the viscosity has been modeled through a phenomenological model composed by a mixture law of the shear viscosities of the reactants (polyol, isocyanate and water), a power law introducing the shear-thinning behavior and a polynomial equation representing the contribution of the rate of gas creation in the foam. The authors have reported that the needed material parameters for this model were not available. The chemical reactions were modeled by two second order kinetics models. By monitoring the temperature and the foam height and by using values published in the literature, the kinetic parameters have been identified.

For an elementary representative foam volume composed by a set of gas bubbles in a polymer shear-thinning viscous fluid matrix, Bikard et al. [12] have used a finite element method to follow the evolution of macroscopic parameters such as porosity. The needed parameters for the blowing reaction have been arbitrarily estimated while for the gelling reaction, the authors have used the results of Dimier et al. [18]. Dimier et al. [18] have studied the kinetics of the gelling reaction and the rheological behavior for polyurethane. They have used the differential scanning calorimetry (DSC) to estimate the kinetic parameters and the small amplitude oscillatory shear rheometry to identify the parameters of the adopted rheological model through nonlinear regression based on error minimization. Bikard et al. [13] have studied the macroscopic aspect of the foaming process for flexible polyurethane foam by presenting the foam as a homogeneous compressible viscous fluid. They have added the difference of pressure between the gas and the polyurethane as a factor of expansion in addition to the gas generated. This reaction has been modeled by an *n*th order kinetic model and the gelling reaction by a Piloyan law [19]. The evolution of the viscosity has been modeled by a phenomenological equation whose parameters have been taken from the literature. By using a dynamic rotational rheometer with parallel-plate system, Bouayad et al. [14] have carried out an experimental work to identify the kinetic parameters of the two main reactions. The authors have monitored the evolution of the elastic modulus G' and the loss modulus G'' in time for different temperatures. They have shown that the radial expansion due to the creation of gas can be neglected and thus the results can be exploited directly. They estimated the needed kinetic parameters and their dependency on temperature. Due to experimental difficulties caused by the height reactivity of the chemical reactions, the authors used a set of delaying chemical agents and they supposed that these agents have not a great influence on the results. However, the time characteristics of the different reactions were highly increased. The simulation of the foaming process using a physical and chemical blowing agent has been studied by Geier et al. [20] by using the volume-of-fluid (VOF) method implemented in the commercial code FLUENT. The authors have modeled the gelling and the blowing reactions by a second-order kinetic model and a first-order kinetic model respectively based on the work of Baser and Khakhar [11, 15]. The foam density has been supposed to be function of the temperature, the pressure, the rate of the blowing reactions (for water and physical blowing agent). The evolution of the foam viscosity has been described by an empirical model depending on temperature, conversion of isocyanate and shear rate. To determine the heat of each reaction, they monitored the temperatures of the foam obtained with three different polyurethane formulations. The first formulation was prepared without blowing agent (neither chemical nor physical agent) and was assumed to be representative of the gelling reaction. For the second formulation, the water was added as the blowing agent. For the third formulation, the water was replaced by the physical blowing agent. Using the results of these three reactions, the authors have solved a system of three linear equations to determine the heat generated during each reaction. The kinetic parameters have been determined using an adiabatic temperature rise method presented by Lipshitz and Macosko [21]. The evolution of the rate of the gelling reaction with time has been calculated by using the temperature evolution for the first formulation. The rate of the reaction of isocyanate with water has been calculated by using the evolution of the volume of the foam for the second formulation.

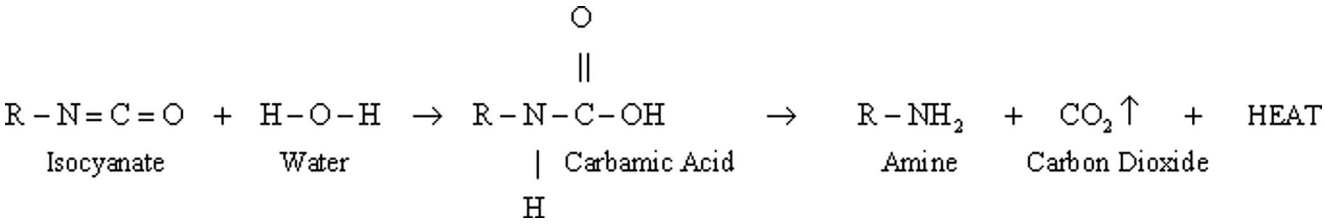

Fig. 1 Blowing reaction

Either for a microscopic or macroscopic approaches, the determination of the parameters of the model is extremely important for the accuracy of the polyurethane foaming simulation. However, this task necessitates an extensive experimental work to characterize the chemical, thermal and rheological behavior of the polyurethane foam. The determination of the parameters of the model, the calibration and the validation of the final model became complicated. In the present work, we propose an inverse identification procedure aiming at determining all the parameters of the model by using experimental results from dynamic rotational rheometer with parallel-plate system and FOAMAT system coupled with foaming simulations by using the finite pointset method (FPM) introduced by Kuhnert [22].

In the following section the necessary fundamentals of polyurethane chemistry and rheology are presented. Afterwards, the numerical simulation model is introduced including governing equations and numerical implementation in the FPM framework. The experimental methods and the parameters identification procedure are then presented. The last section is devoted to the results and discussion. First, the analysis of the model response on the FOAMAT system is detailed. Then, the model is validated against experimental short shot foam obtained from a panel mold cavity. Finally, the mold filling of an automotive underlay carpet cavity is analyzed and compared to experimental results obtained from industrial tests.

Theoretical model

Polyurethane foam is considered at a macroscopic scale, as a homogeneous continuous medium, whose rheological behavior depends on temperature. The evolution of the PU foam properties mainly depends on its structure at the macromolecular level (state changes, interaction between components…). There is a strong thermo-rheological coupling: the increase of temperature inside the foam leads to the change of its rheological behavior, and thus its microstructure, up to its gelling. There are two main reactions in the polyurethane foam formation: polymerization or gelling reaction and blowing reaction. The gelling process leading to the formation of polyurethane increases both viscosity and temperature of the foam because the reaction between isocyanate and polyol is highly exothermic. The polyurethane foam is expanded by the creation of the carbon dioxide gas and its diffusion into the nucleated bubbles. At the end of this process, the final cellular structure of the polyurethane foam is created. Kinetic parameters for the gelling and blowing reactions are usually assumed to be independent of each other. It is generally assumed that the foam expansion is the result of the generation of the carbon dioxide which is controlled by the water–isocyanate reaction.

Blowing reaction

The first step of the model of blowing reaction involves the reaction of an isocyanate group with water to yield a thermally unstable carbamic acid which decomposes to give an amine functionality, carbon dioxide and heat. In the second step (Fig. 1), the newly formed amine group reacts with another isocyanate group to give a disubstituted urea and additional heat is generated. The total heat generated from the blow reaction along with the carbon dioxide released in the first step serve as the principal source for blowing the foam mixture.

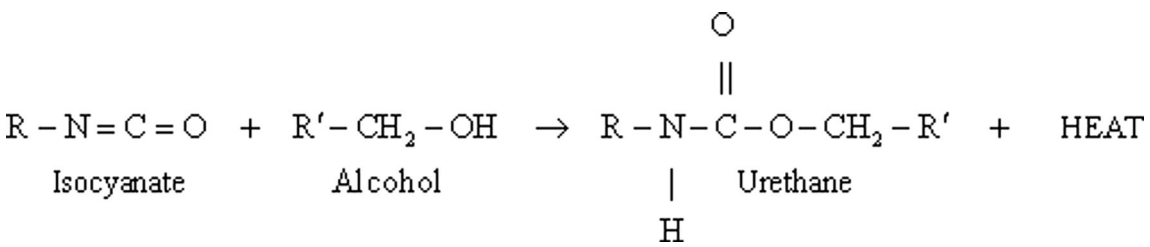

Fig. 2 Gelling or cross-linking reaction

This reaction is governed by chemical kinetics and is supposed to follow a Piloyan law [19]:

$$\frac{d\alpha}{dt} = \frac{1}{\tau_\alpha}\alpha^{m_\alpha}(1-\alpha)^{n_\alpha} \quad \text{with} \quad \alpha = \alpha_0 \quad \text{at} \quad t = t_0 \tag{1}$$

where α is the chemical conversion rate of CO_2 creation, τ_α is the characteristic time of the reaction and n_α is the exponent of the reaction. In this work, we suppose that this reaction is of second order then we have n_α=2−m_α.

Gelling reaction

The gelling reaction, also sometimes called the polymerization reaction, involves the reaction of an isocyanate group with an alcohol group to give a urethane linkage as shown in Fig. 2. Since polyurethane foams usually utilize polyfunctional reactants this reaction leads to the formation of a cross linked polymer.

If molecular diffusion is neglected, the kinetic equation of gelling reaction can also be represented by a Piloyan law [19]:

$$\frac{d\beta}{dt} = \frac{1}{\tau_\beta}\beta^{m_\beta}(1-\beta)^{n_\beta} \quad \text{with} \; \beta = \beta_0 \quad \text{at} \quad t = t_0 \tag{2}$$

where β is the chemical conversion rate of the gelling reaction, τ_β is the characteristic time of the reaction and m_β, n_β are the exponents of the reaction. As for the blowing reaction, we suppose that the gelling reaction is of second order then we have n_β=2−m_β.

Viscosity model

The viscosity is one of the most important parameters for the simulation of the foaming process. Thus, an accurate viscosity model should be used for an accurate analysis of foaming process. The foam is considered as a Newtonian fluid whose viscosity depends on the temperature (T), the chemical conversion rate of the gelling reaction (β) and the porosity of the foam (ϕ):

$$\eta(T,\phi,\beta) = \eta_0(T)f(\phi)g(\beta) \tag{3}$$

The thermo-dependence of the viscosity is usually written as Arrhenius type law:

$$\eta(T) = \eta_0 \exp\left(\frac{E_\eta}{R}\left(\frac{1}{T}-\frac{1}{T_0}\right)\right) \tag{4}$$

where R is ideal gas constant and E_η is the activation energy, η_0 is the viscosity of the mixture (isoyanate and polyol) at a reference temperature (T_0=23 °C) before their reaction.

The porosity-dependence of viscosity is derived from the study of phenomena of emulsion when the interaction between the dispersed bubbles cannot be neglected (substantial concentration of gas). The most general expression can be represented in an exponential form [23]:

$$f(\phi) = \exp\left(\frac{k}{\phi}\right) \tag{5}$$

with

$$k = k_0 \exp\left(\frac{E_k}{R}\left(\frac{1}{T}-\frac{1}{T_0}\right)\right) \tag{6}$$

where k_0 and E_k are the model parameters.

The conversion-dependent viscosity is obtained by the application of the percolation model to gelling [24]:

$$g(\beta) = \left(\frac{\beta_{gel}}{\beta_{gel}-\beta}\right)^{a(T)\beta+b(T)} \tag{7}$$

with:

$$a(T) = a_0 \exp\left(\frac{E_a}{R}\left(\frac{1}{T}-\frac{1}{T_0}\right)\right) \tag{8}$$

$$b(T) = b_2 \; T^2 - b_1 T + b_0 \tag{9}$$

where β_g is the conversion at gel point, E_a, a_0, b_0, b_1 and b_2 are model parameters.

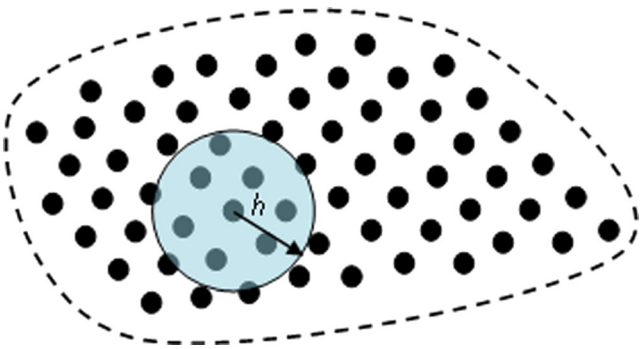

Fig. 3 Particle distribution and definition of neighbor points (smoothing length h)

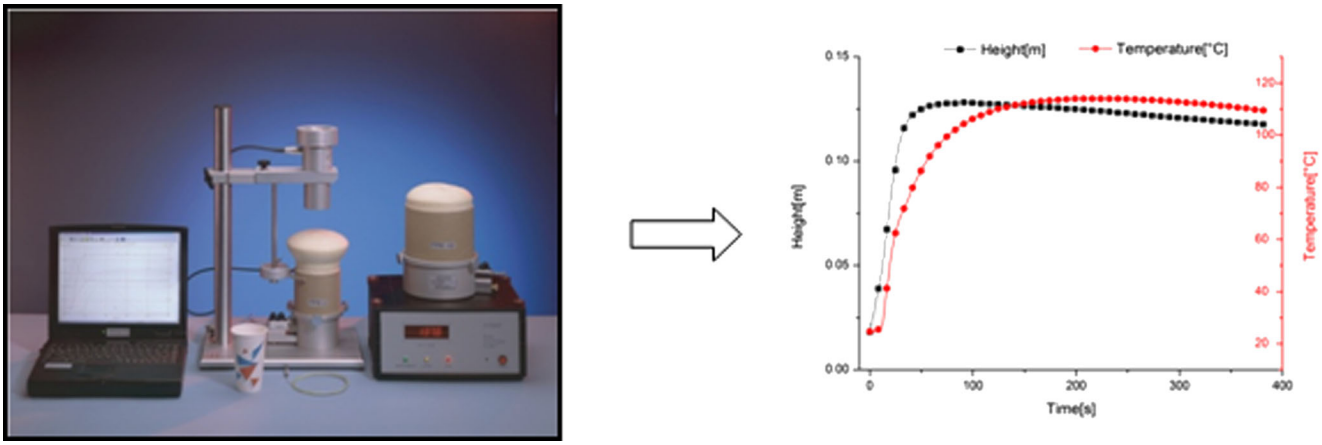

Fig. 4 FOAMAT system and typical curves obtained for foam height and temperature

Numerical model

Governing equations

For numerical investigation of mold filling, foam is considered as pseudo-homogeneous fluid and modeled as a continuum with the assumption of ideal mixing. It is assumed that the continuum is a generalized Newtonian fluid whose constitutive equation is governed by the foam rheology. The general governing equations for compressible Newtonian fluid with Stokes' hypothesis include the mass conservation equation, momentum conservation equation, and the energy conservation equation.

Mass conservation equation

The conservation of mass is written as:

$$\frac{d\rho}{dt} + \nabla\cdot(\rho\mathbf{v}) = 0 \tag{10}$$

where $\mathbf{v}$ is the velocity field, ρ is the mass density and ∇ is the divergence operator.

Bikard et al. [13] proposed a homogenized model for the mixture by introducing the porosity ϕ (volumetric ratio of gas) and by using the foam growth model introduced by Amon and Denson [3, 4]:

$$\nabla\cdot\mathbf{v} = \frac{1}{1-\phi}\frac{d\phi}{dt} \tag{11}$$

$$\frac{d\phi}{dt} = \phi(1-\phi)\left(\frac{1}{\alpha}\frac{d\alpha}{dt} + \frac{1}{T}\frac{dT}{dt}\right) \quad \text{with} \quad \phi = \phi_0 \quad \text{at} \quad t = t_0 \tag{12}$$

where α is the conversion rate of CO_2 creation.

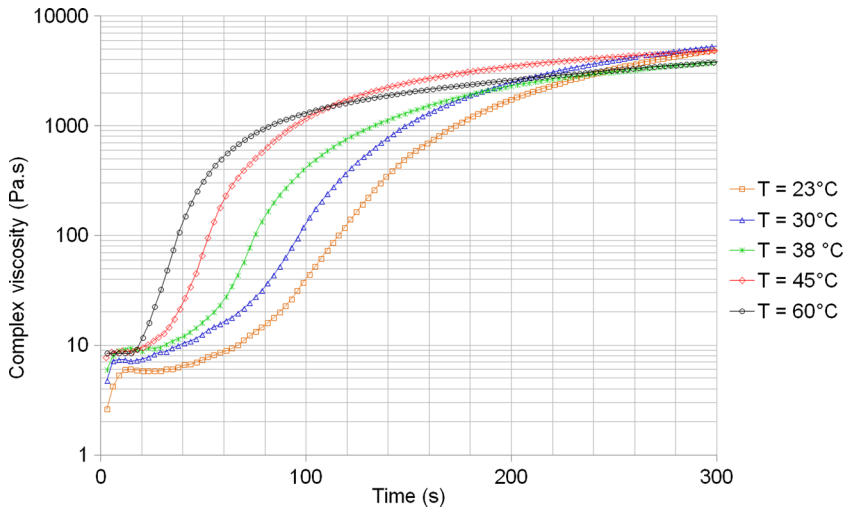

Fig. 5 Complex viscosity evolution for different temperatures

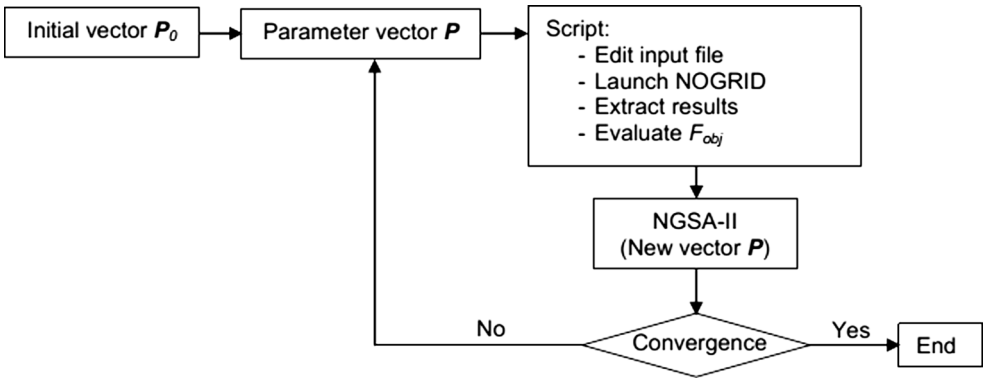

Fig. 6 Workflow of the optimization procedure

Momentum conservation equation

The conservation of momentum is given by:

$$\frac{d(\rho \mathbf{v})}{dt} = -\nabla p + \nabla \cdot \mathbf{s} + \rho \mathbf{g} \tag{13}$$

where $\boldsymbol{g}$ is the gravity vector and $\boldsymbol{s}$ is the deviator part of the stress tensor given by:

$$\mathbf{s} = \eta(T, \phi, \beta)\left[(\nabla \mathbf{v}) + (\nabla \mathbf{v})^T\right] \tag{14}$$

where the superscript T indicates the transpose of tensor and $\eta(T,\phi,\beta)$ is the viscosity defined in Eq. (3).

The mixture density is expressed as a function of the porosity ϕ as follows:

$$\rho = (1-\phi)\rho_{\mathrm{PU}} + \phi \rho_{\mathrm{CO2}} \tag{15}$$

where ρ_{PU} is the density of the polyurethane and ρ_{CO2} is the density of the CO_2 gas.

The velocity field $\mathbf{v}=\mathbf{0}$ is imposed on the mold walls.

Energy conservation equation

The conservation of energy is given by:

$$(\rho C_p)\frac{dT}{dt} = \nabla^T \cdot (k \nabla T) + \nabla^T \cdot (\mathbf{s} \cdot \mathbf{v}) - (\nabla^T \mathbf{s}) \cdot \mathbf{v} + p \cdot (\nabla^T \cdot \mathbf{v}) + Q \quad \text{with} \quad T = 23^{\circ}\mathrm{C} \quad \text{at} \quad t = t_0 \quad T = 23^{\circ}\mathrm{C} \quad \text{on the mold walls} \tag{16}$$

where T is the temperature, $C_p=(1-\phi)C_{PU}+\phi C_{CO2}$ is the thermal capacity of the mixture, $k = (1-\phi)k_{PU} + \phi k_{CO_2}$ is the thermal conductivity of the mixture and Q is a source term due to the exothermic effect of CO_2 creation and gelling reactions which can be expressed as:

$$Q = \Delta H_\beta \frac{d\beta}{dt} + \Delta H_\alpha \frac{d\alpha}{dt} \tag{17}$$

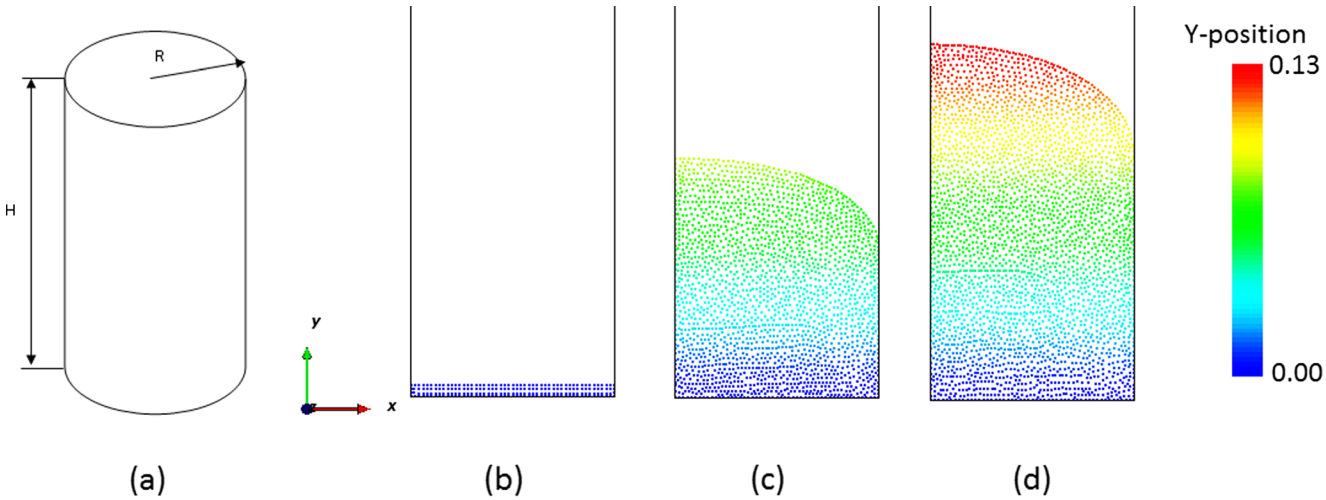

Fig. 7 Foam expansion in a FOAMAT cylinder: **a** problem geometry, **b** initial front position, **c** front position at t=30 s, (d) front position at t=180 s

Table 1 Initial and final values of the model parameters identified by inverse analysis

Parameters	Initial values (min–max)	Identified values
τ_α [s]	7–9	8.5
m_α	0.6–0.8	0.73
τ_β [s]	100–120	113.8
m_β	0.7–0.9	0.82
E_η [J.mol^{-1}]	1.7 10^4–2.0 10^4	1.89 10^4
k_0	−0.09 to −0.07	−0.074
E_k [J.mol^{-1}]	8 10^4–10 10^4	8.1 10^4
a_0	100–120	100.4
E_a [J.mol^{-1}]	9.0 10^3–11.0 10^3	1.06 10^4
b_0	225–275	248.2
b_1	1.8–2.2	2.07
b_2	0.0037–0.0045	0.0042
ΔH_α [J.m^{-3}]	4.5 10^6–5.5 10^6	5.02 10^6
ΔH_β [J.m^{-3}]	1.6 10^6–2.0 10^6	1.8 10^6

where ΔH_α is the enthalpy of the reaction of isocyanate with water and ΔH_β is the enthalpy of the gelling reaction.

Numerical implementation

As an alternative to grid-based numerical methods such as finite difference, finite element and finite volume methods, the meshless formulation was developed from the 1970s with the emergence of SPH (smoothed particle hydrodynamics) method which was originally dedicated to the study of astrophysical problems [25]. To extend the application of this formulation to study others classes of problem, a set of methods based on this approach have been developed [26]. These methods tried to avoid the main disadvantages of the SPH formulation such as tensile instability, interpolation consistency and especially the boundary conditions implementation. For the last one, several solutions have been proposed such as the ghost particle approach [27], the Lagrangian multiplier method [28], transformation method [29] and boundary singular kernel method [30]. More details for these methods are presented in [26].

As an amelioration of the finite point method developed by Oñate et al. [31], Kuhnert [22] presented the finite pointset method (FPM). For this method which uses the moving least squares approach, the boundaries are presented by a set of fixed boundary particles and the boundary conditions are imposed on these particles.

The FPM method has been successfully applied to a set of industrial applications such as glass forming [32], cutting simulation [33] and fluid structure interaction [34]. Using FPM, the fluid domain is discretized by finite number of Lagrangian particles which move with fluid velocity and carry along with them all fluid properties such as density, viscosity, velocity, temperature and so on (Fig. 3). The list of neighbor points is determined for each point at each time step through the definition of a zone of influence. Indeed, a smoothing length h which can be function of time and space (Fig. 3) is attached to each particle and it is used to create an interpolation function using a Moving Least Square (MLS) method.

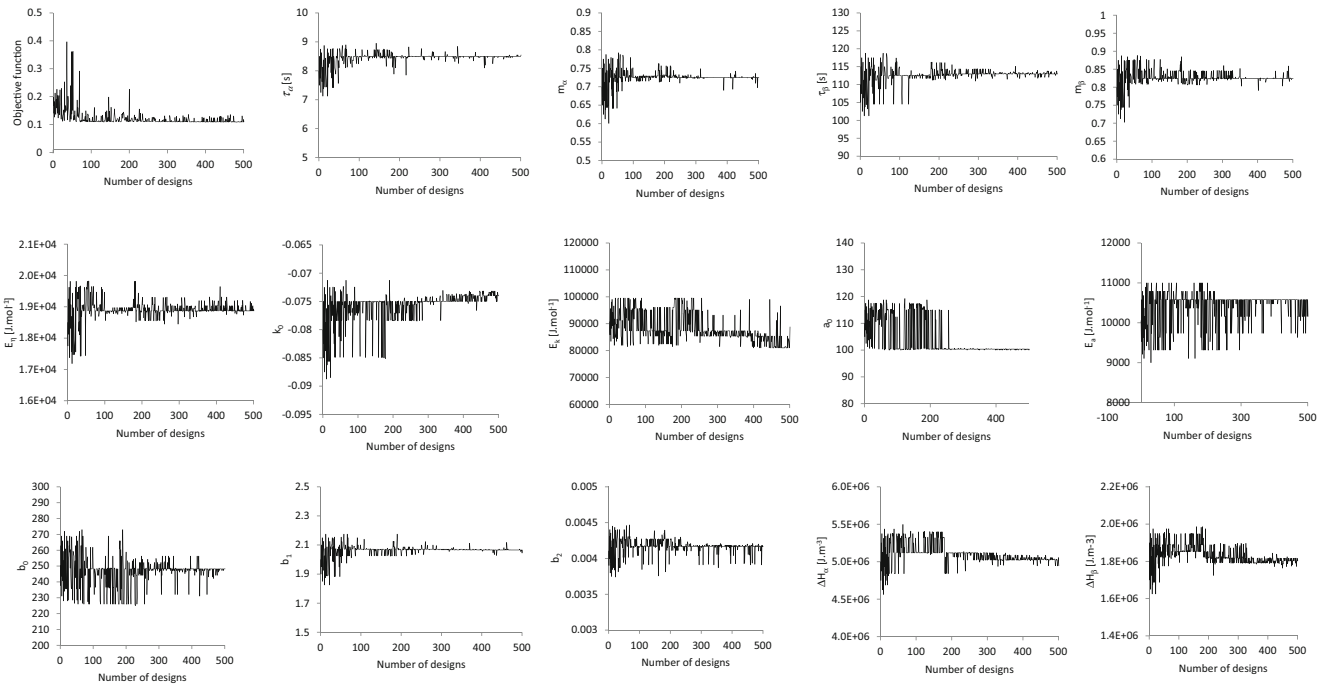

Fig. 8 Evolution of the objective function and model parameters during the identification procedure

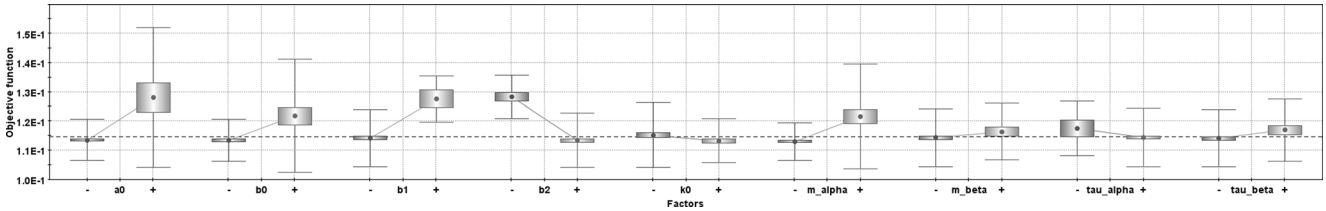

Fig. 9 Main effects of the different parameters on the objective function

The simulation of the foaming process in industrial applications is characterized by complex mold shapes. FPM is a grid-free (or meshless) method which, in contrast to classical numerical methods does not require a grid or a mesh whose generation takes a long time for complex geometries. Furthermore, this work is an initial step to simulate the foaming process in an open mold technique. This technique consists in using a moving injector to inject the mixture at the bottom of an open mold. After the injection step, the injector is removed and the mold is closed. The use of a grid-based method necessitates the meshing of a large domain to take into account the injector and the moving part of the mold thus increasing significantly the simulation time.

The adopted model is implemented in the NOGRID-points software. We have to solve the set of differential equations defined by conservation equations with appropriate boundary conditions. This system is highly coupled and non-linear. Thus, a splitting technique is used to decrease the degree of complexity. On one time step, knowing α, β and T, the velocity and pressure fields are determined through a least-squares particle method; the velocity is then used to compute temperature and reactions' rates.

The pressure–velocity equations are solved by applying an implicit projection method [35], which is based on the least-squares particle method used in FPM [22].

Identification of model parameters

To perform an accurate simulation, it is very important to characterize the chemical, thermal and rheological behavior of the polyurethane foam. However, the constitutive models are very complex due to the coupling between chemical, thermal and rheological phenomena, and usually require a significant amount of experimental data to determine the parameters of the model and, therefore, to calibrate and validate the final model. In this study, we propose an inverse method aiming at determining chemical, thermal and rheological properties associated to the foam expansion model. The main idea is to identify a set of parameters such that, for a desired range of operating conditions, the model outputs match well the experimental outputs, when both are submitted to the same inputs.

Experimental characterization

Using a foam qualification system FOAMAT (Format Messtechnik GmbH), the foam rise and the reaction temperature are monitored during the foaming process on a cylindrical cardboard test tube (Fig. 4).

The determination of the foam height in the Foamat and the temperature evolution are carried out using respectively an ultrasonic sensor and a thermocouple fixed in the center of the cylindrical cardboard test tube.

The evolution of the viscosity during the foaming process has been measured using AR2000ex rotational rheometer (TA Instruments) using parallel plate system. The experimental protocol is similar to that adopted by Bouayad et al [14] without any delaying chemical agent to ensure that the obtained results describe the true time evolution of the viscosity. The experiments have been carried out for five different temperatures (23, 30, 38, 45 and 60 °C) and typical results of complex viscosity (η^*) are plotted in Fig. 5.

During the experiments the temperature is controlled by the system and is supposed to be homogeneous. These experiments have been achieved using a fixed frequency of 1Hz in order to have enough information about the evolution of the viscosity (by using low frequencies we have few information due to the high reactivity of the used formulation) and to avoid the tear of the foam structure for high frequencies. By using this frequency, the influence of the elongational flow can be neglected [14].

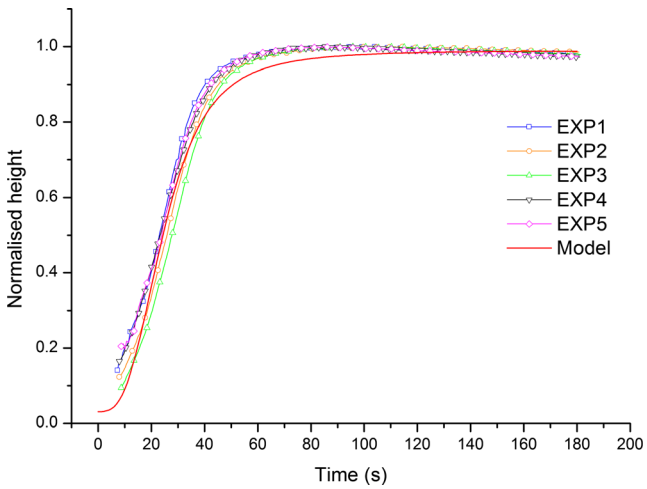

Fig. 10 Comparison between experimental and numerical foam expansion in a FOAMAT cylinder

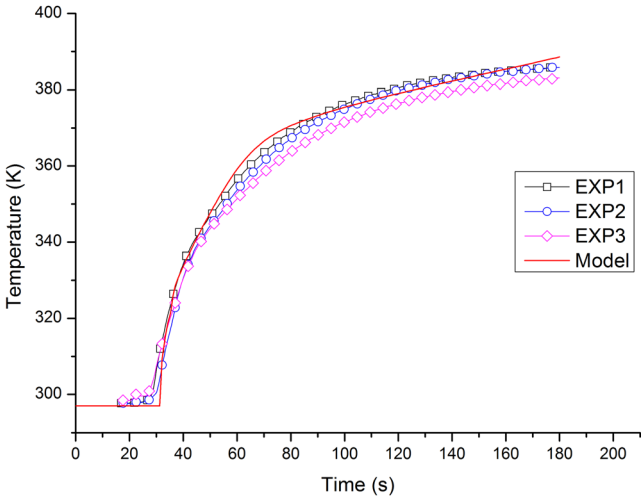

Fig. 11 Comparison between experimental and numerical results core foam temperature

The obtained results present the rheological behavior of the foam during and after the foaming process. In fact, the foam is considered as a viscous fluid before the gel point and after this point it is characterized by a high increase in the viscosity. In this work we suppose that the viscosity is described by a percolation model defined in Eq. (7). Thus, only the first parts of the experimental curves are exploited and the viscosity is supposed to become infinite after the gel point supposed to be in the inflection point of the complex viscosity curve as presented in Fig. 5 [36].

Identification procedure for the model parameters

The inverse method presented in this paper consists in determining the parameters by comparing the computed quantities (foam height, reaction temperature and viscosity) to those measured experimentally. The unknown material parameters in the numerical model (τ_β, m_β, τ_α, m_α, E_η, E_k, E_a, k_0, a_0, b_0, b_1 , b_2, ΔH_α and ΔH_β) are iteratively tuned so as to match the experimentally measured and the numerically computed quantities as closely as possible. The objective function is defined as:

$$F_{obj} = min\left\{\frac{1}{N_h}\sum_{i=1}^{N_h}\left[p_h\left(h(\mathbf{P},t_i)-h_{\exp}(t_i)\right)^2\right] + \frac{1}{N_T}\sum_{i=1}^{N_T}\left[p_T\left(T(\mathbf{P},t_i)-T_{\exp}(t_i)\right)^2\right]\cdots \right.$$
$$\left. \cdots + \frac{1}{N_\eta}\sum_{i=1}^{N_\eta}\left[p_\eta\left(\eta(\mathbf{P},t_i)-\eta_{\exp}(t_i)\right)^2\right]\right\} \quad (18)$$

where $\boldsymbol{P}$ is the vector of the unknown material parameters, subscripts h, T and η refer to foam height, temperature and viscosity respectively, N_h, N_T and N_η are the numbers of experiment points, t_i is the time corresponding to the experimental point i and p_h, p_T and p_η are weighting parameters.

The workflow of the optimization process is shown schematically in Fig. 6:

- A parameter vector and a parameter file are defined.
- An initial set of designs to be evaluated is generated.
- A script is used to: read the parameter file, edit the input file, launch NOGRID points software, extract the necessary results and evaluate the objective function
- The overall optimization process is driven by NSGA-II algorithm (Non-dominated Sorting Genetic Algorithm II) [37].

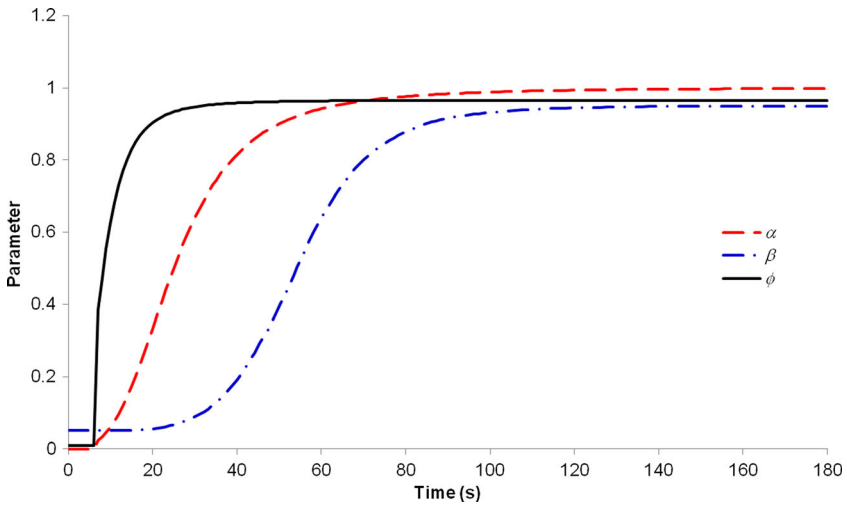

Fig. 12 Chemical conversion rates and porosity evolution

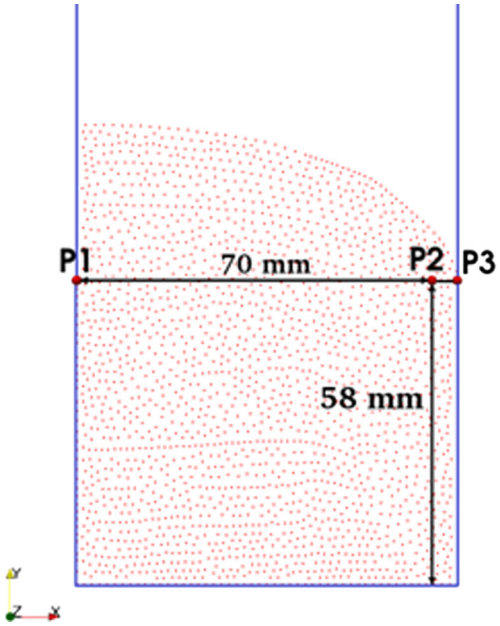

Fig. 13 Particle distribution at t=30s

The NSGA-II algorithm used in this work has been proposed by Deb et al. [37] and it consists in the generation of an initial random set of parameter vectors. For each vector the values of the material parameters is chosen between the minimal and the maximal values assigned to every parameter. After achieving the identification procedure using all the parameter vectors generated in the initial set, combinations of those providing the best results for the minimization of the objective function are used to generate a new set. This technique is repeated until having the parameter vector which provides the minimum difference between the numerical and experimental results.

The identification procedure in this work is divided into two principal stages: the initialization stage and the optimization stage.

The initialization stage

In this stage, we start by identifying the material parameters τ_α and m_α related to the blowing reaction using the foam height results. To do so, we exploited the experimental results of five tests achieved in the same conditions and we used Eq. (18) with p_h=1 and p_T=p_η=0.

The next step is the identification of the material parameters corresponding to the initial viscosity temperature dependence (E_η) and the contribution of the blowing reaction in the evolution of the viscosity (k_0, E_k). As presented by Bouayad et al [14], this contribution is manifested in the beginning of the foaming process. During this step we fixed the material parameters τ_α and n_α and we exploited the first zone of the viscosity curves (<20 s) in Fig. 5 and we used a modified viscosity model presented by the Eq. (19).

$$\eta(T,\phi,\beta) = \eta_0(T) f(\phi) \tag{19}$$

The identification is carried out using Eq. (18) with p_η =1 and p_T=p_h =0.

The third step in the initialization stage is the identification of the material parameters related to the contribution of the gelling reaction to the evolution of the viscosity (τ_β, m_β, E_a, a_0, b_0, b_1 , b_2). To do so, we fixed the already determined parameters and we exploited the whole viscosity curves. The identification is carried out using Eq. (18) with p_η =1 and p_T= p_h =0 and the viscosity model given in Eq. (3).

The last step concerns the identification of the enthalpies of the two reactions. The experimental curves used in this step have been obtained by monitoring the temperature evolution in the center of the cylindrical cardboard test tube for three tests carried out in the same experimental conditions. We used Eq. (18) with p_T =1 and p_η=p_h =0.

The optimization stage

Due to the complexity of the foaming process, all model parameters have been optimized simultaneously. The material parameters obtained in the initialization stage (Table 1) are used to generate a design of experiment in a range defined by ±20 % of these values. Then an identification process taking in

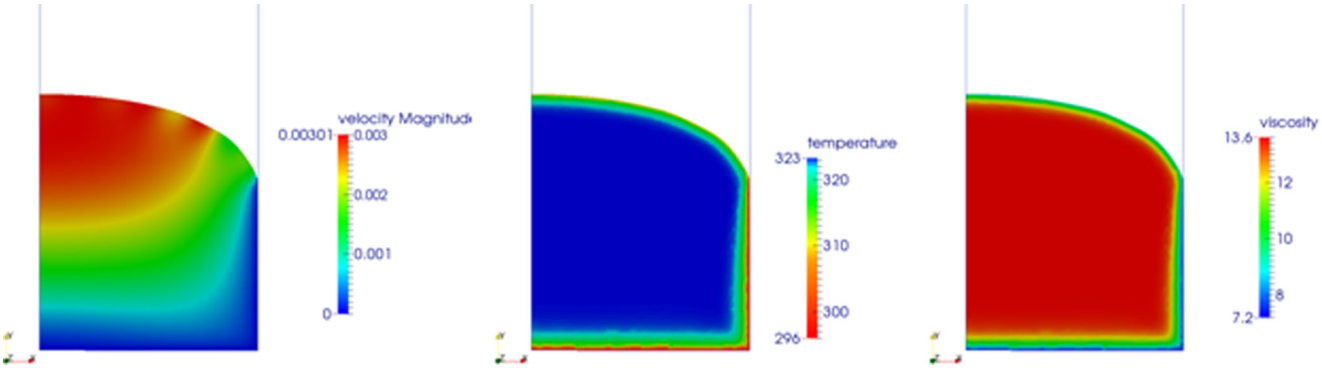

Fig. 14 Isovalue of: **a** particle velocities, **b** foam temperature and (**c**) foam viscosity at t=30s

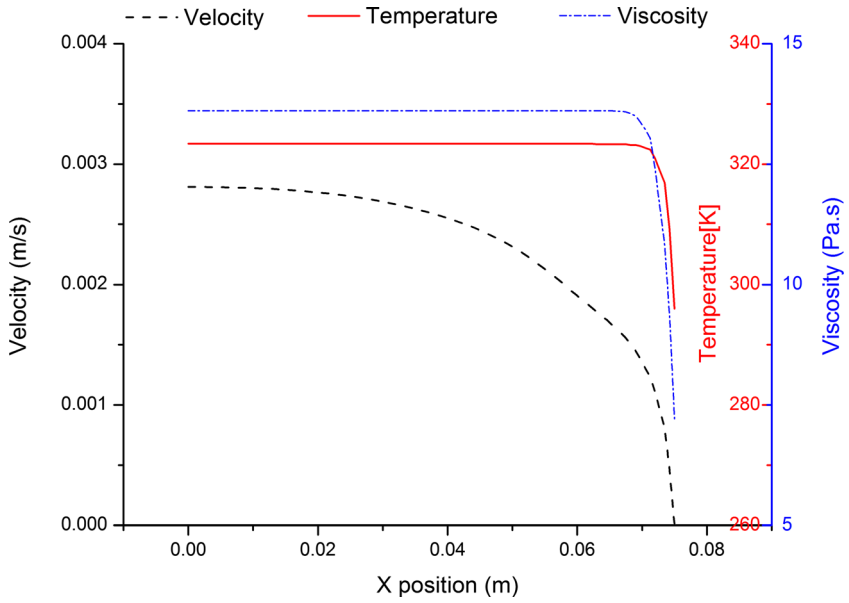

Fig. 15 Profiles of particle velocities, foam temperature and foam viscosity

consideration the coupling between chemical, thermal and rheological phenomena and using the experimental results of the foam height, the temperature and the viscosity has been achieved.

Results and discussion

Results of the identification the model parameters

In order to identify the parameters of the model, the simulation of foam expansion in a FOAMAT cylindrical cup of height H=250 mm and radius R=75 mm is defined in Fig. 7(a). In order to reduce the simulation time, we have used the axi-symmetric model defined in Fig. 7(b).

A no-slip condition is imposed ($\mathbf{v}$=0) at the cylinder walls. At the initial time step, the mixture occupies the region defined in Fig. 7(b) corresponding to the amount of the mixture initially introduced into the cup. Figure 7(c–d) show the front positions of the foam after t=30 s of foaming and at the end of expansion corresponding to t=180 s.

The parameters of the model used for this simulation are obtained by using the identification procedure defined in the precedent section and are summarized in Table 1.

As shown in Fig. 8, the objective function decreases progressively during the identification and converges to a minimum. The evolution of the model parameters during the identification procedure are also shown in Fig. 8. After an important fluctuation in early stage of the identification procedure, the parameters converge to their final values. These figures show that a slight variation in the parameters do not increase the objective function. We have also presented in Fig. 9 an analysis of the main effects of the different parameters on the objective function. We can notice that the

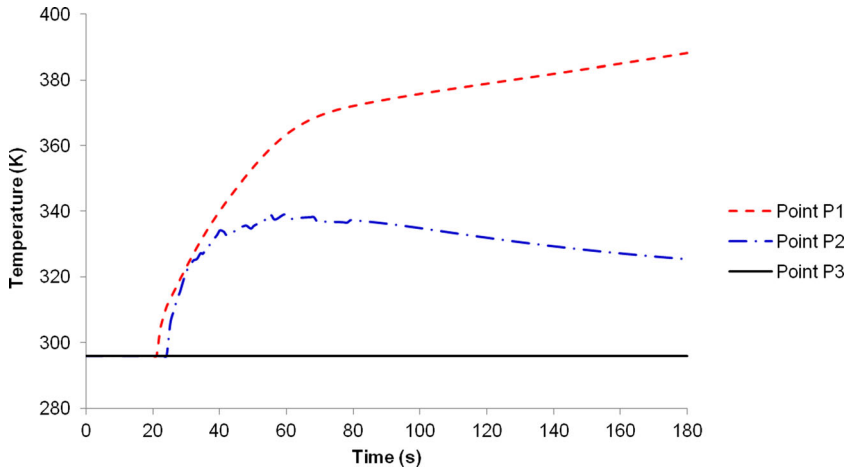

Fig. 16 Evolution of the foam temperature of P1, P2 and P3 during foaming

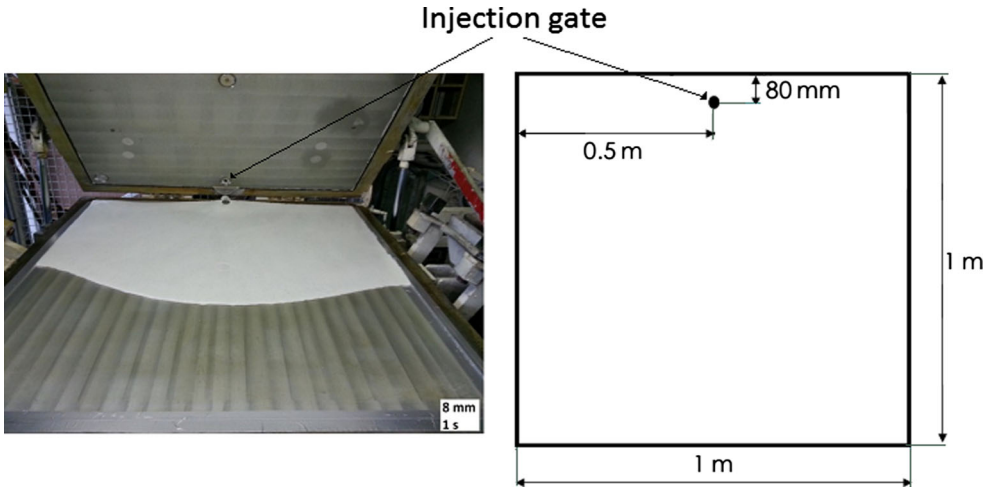

Fig. 17 Experimental panel mold used for the validation of the model

parameter k_0 do not have much influence in the process , the parameter a_0 has the biggest influence and the other parameters have more or less influence.

Figures 10 and 11 show the comparisons between experimental and numerical foam expansion and core foam temperature in a FOAMAT cylindrical cup respectively. In Fig. 10 the

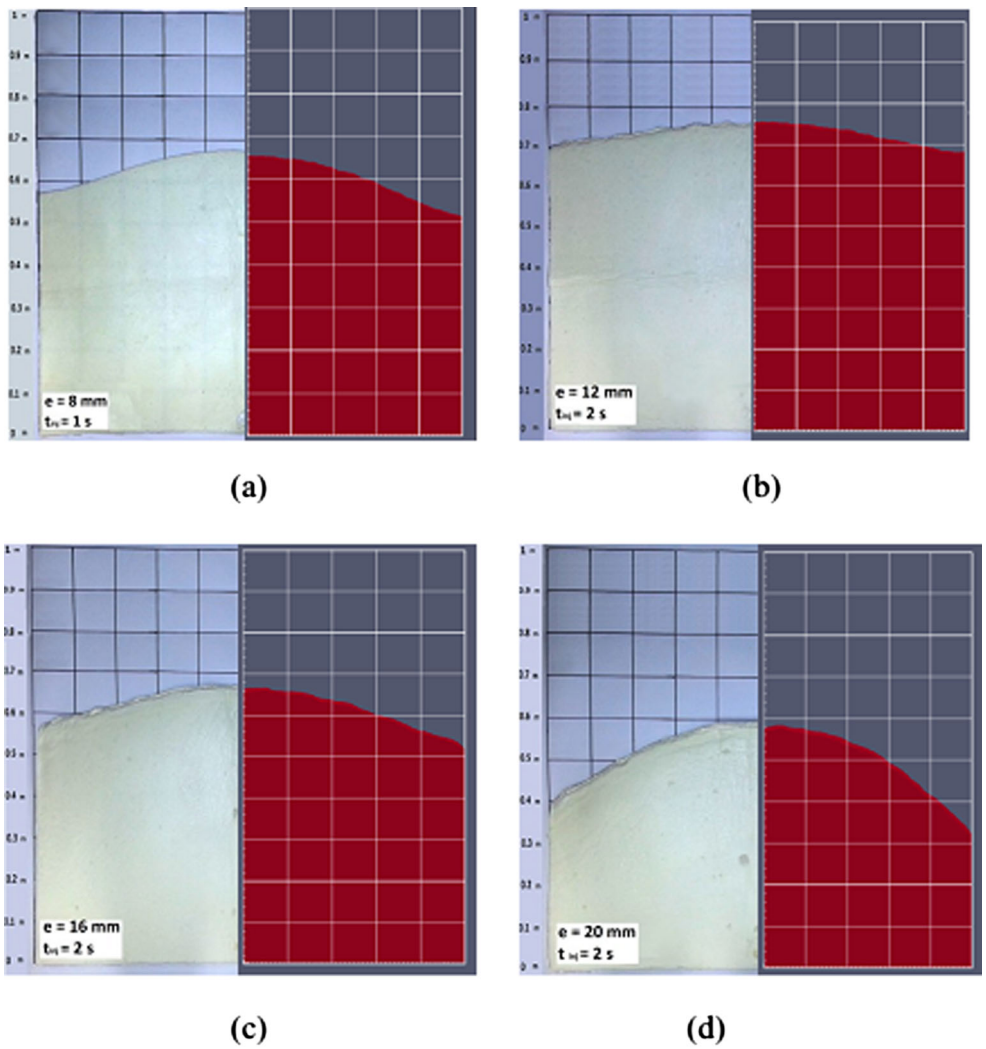

Fig. 18 Comparison between experimental and numerical results for the foaming process of a panel cavity for thicknesses: **a** 8 mm, **b** 12 mm, **c** 16 mm and **d** 20 mm

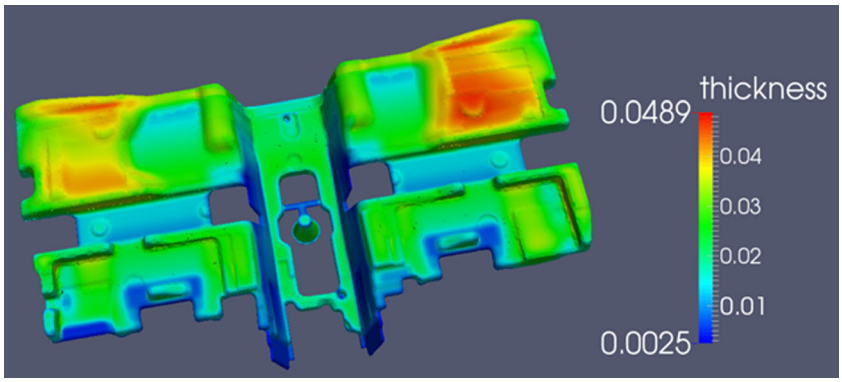

Fig. 19 Three dimensional shape of the underlay carpet with its thickness distribution

five experiments have been carried out in the same conditions and the normalized height represents the height in the center of the expanded foam divided by the maximum height reached at the end of expansion.

The numerical results are very close to the experimental ones, showing that the proposed identification procedure gives a set of parameters enabling accurate foaming simulations.

The chemical conversion rates of gas creation and gelling reactions as well as the porosity are plotted in Fig. 12. This figure shows that the maximum porosity of 95 % is reached around 60 s and the gas creation and gelling reactions conversion rates reach their maximum values $\alpha_{max}=1$ and $\beta_{max}=\beta_{gel}=0.95$ respectively around 120 s. These results show that the expansion ends around 60 s but the foam is not completely gelled.

Using Eq. (15) and the value of the maximum porosity, we deduce that the final density is approximately 50 g/l which is in agreement with the experimental results obtained by dividing the weight of the obtained part by its volume.

The particle distribution representing the foam front position corresponding to a simulation time $t=30$ s is shown in Fig. 13.

The isovalues of the particle velocities, temperature and viscosity of the foam are shown in Fig. 14. We can notice the presence of strong gradients near the walls especially for temperature and viscosity. We have plotted in Fig. 15 the temperature and viscosity profiles through the path defined by the points P1, P2 and P3 which were defined in Fig. 13. We can see that the foam velocity is more important at the center of the cylinder and vanishes

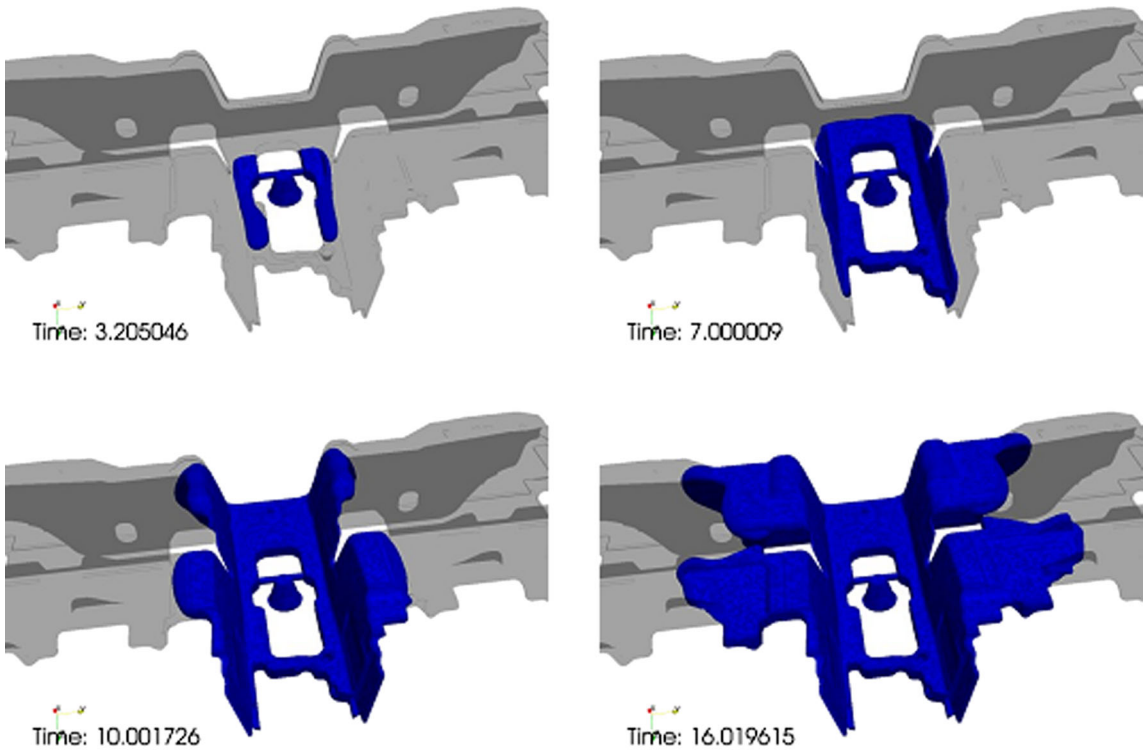

Fig. 20 Flow front positions in the underlay carpet cavity

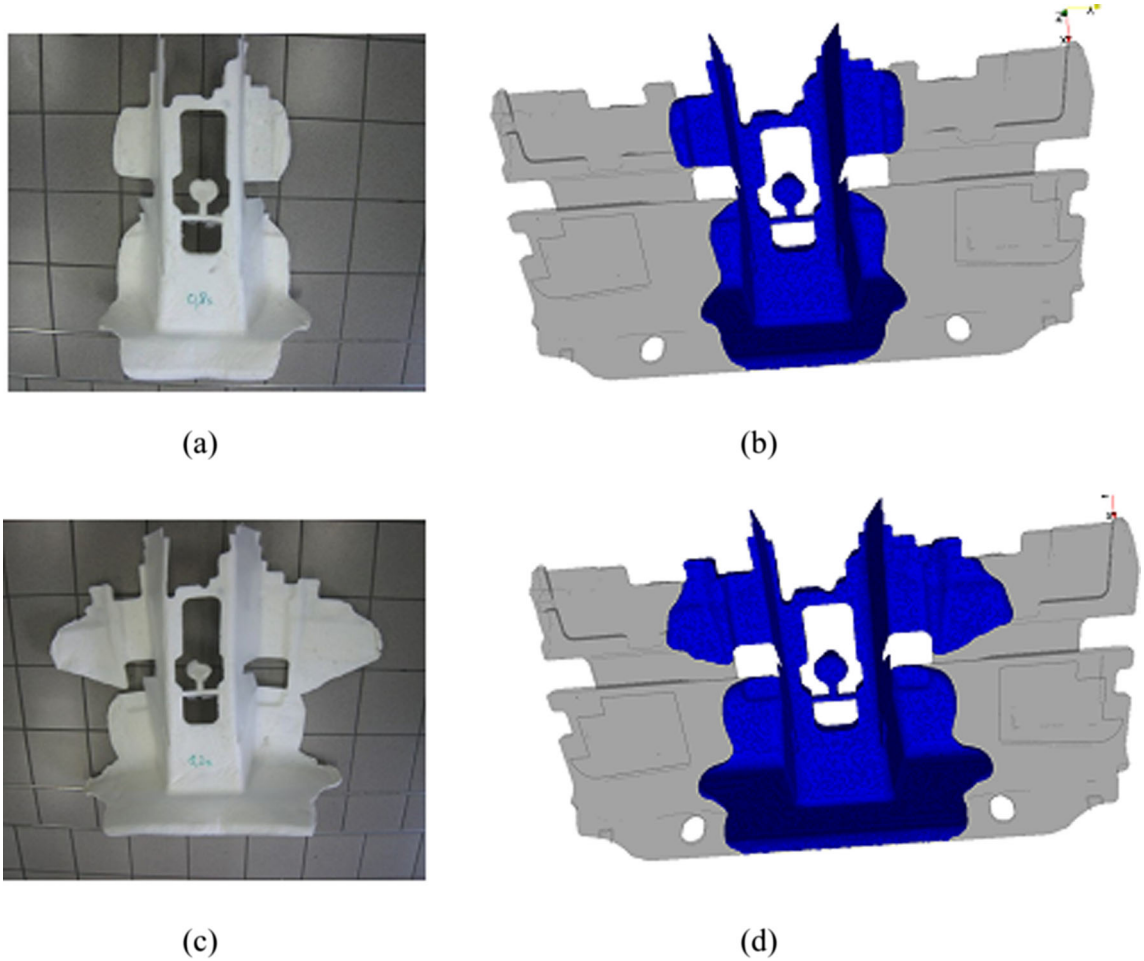

Fig. 21 Comparison between experimental and numerical short shot for the automotive underlay carpet: experimental results (**a** and **c**), calculated results (**b** and **d**)

at the wall boundary in agreement with the imposed boundary conditions. We can notice that the temperature is quasi-homogenous in a wide region of the cylinder and decreases rapidly in a thin transition zone near the wall boundary and the free surface. This narrow region is due to the poor thermal conductivity of the foam and the thermal dissipation is only located near the free surface and the wall boundary. The foam viscosity follows the same tendency as the temperature due to the temperature-dependence of the foam viscosity.

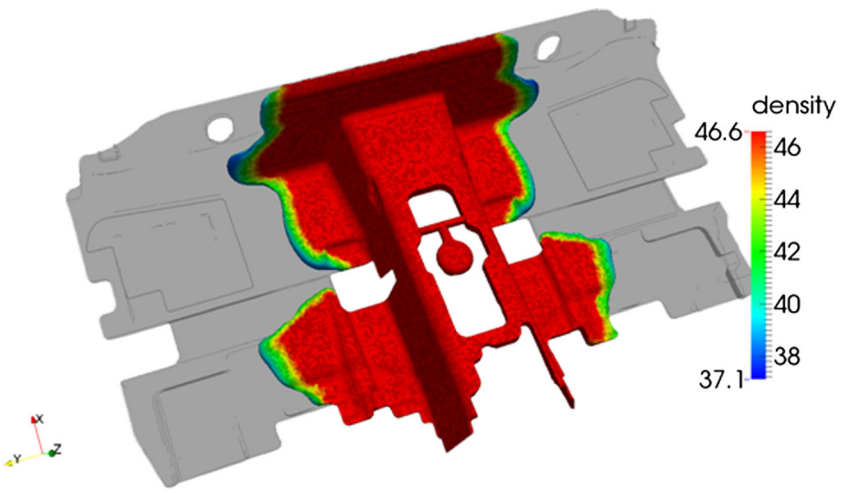

Fig. 22 Density distribution for short shot of the automotive underlay carpet obtained with injection time of 1.2 s

The evolution of the temperature of the points P1, P2 and P3 during foaming simulation is shown in Fig. 16. The temperature of P3 is constant corresponding to the wall temperature defined as T=296 K. We notice that the increase of the temperature of P1 start few seconds before that of P2 because the foam front reaches P1 before reaching P2. The temperature of P1 increases continuously while the temperature of P2 increases until t=60 s then decreases. The temperature increase is due to the reactions heat which is poorly dissipated in the center of the cylinder (P1) because of the low conductivity of the foam, but which is dissipated when the foam reaches the wall boundary (P2).

Validation of panel simulation with short shot foams

To validate the overall model obtained by the inverse identification method, we carried out a set of experimental tests using a square panel mold having different thicknesses. Its dimensions and the position of the injector are shown in Fig. 17. The injected mass flow was fixed to 200 g/s and the panel mold thickness was varied from 8 to 20 mm with an increment of 4 mm. Short shot foams have been obtained by using different injection times avoiding completely filling the mold. To compare the obtained short shots with the foaming simulations, only one half of the mold has been modeled thanks to the symmetry of the problem. All the foaming simulations have been performed under the same conditions as the experimental tests. The obtained results for thicknesses e=8, 12, 16, 20 mm and injection times t_{inj}=1, 2, 2, 2 s respectively are shown in Fig. 18. The left parts of Fig. 18 (a–d) represent the experimental short shots and the right parts represent the corresponding simulations. These results show a good agreement between the experimental and the numerical results. The proposed parameters' identification procedure gives a set of optimal parameters enabling accurate foaming simulations.

Foaming simulation of an automotive underlay carpet

As a practical industrial problem, filling of an automotive underlay carpet is simulated numerically. Three dimensional shape of the part is depicted in Fig. 19 with its thickness distribution. When the part is completely filled the number of particles is 1264725. Unexpanded foam is injected in the mold cavity through an injection gate with a fixed mass flow of 320 g/s. After it is supplied for 3 s, the gate is closed. It is assumed that the cavity has isothermal boundary (T=60 °C) and the gravity is acting in negative z direction. Figure 20 shows the flow front progress at four different times. In the beginning of mold filling unexpanded foam flows out in z directions due to the gravity. After a while, the foam expands to fills up the cavity.

Figure 21 shows a comparison between short shot foam obtained experimentally and by simulation for injection times of 0.8 and 1.2 s. The front positions are almost similar indicating a very good agreement between the experimental and the calculated results. Density distribution for short shot of the automotive underlay carpet obtained with injection time of 1.2 s is shown in Fig. 22. Foam density is dependent on temperature and conversion rate of the blowing agent. The foam density is inversely proportional to conversion rate and temperature. The density is almost constant in the filled region and the lowest density occurs at the flow front.

Conclusion

Polyurethane foaming process has been physically modeled by considering the expansion of a compressible quasi-homogeneous continuous mixture. The computational domain is discretized by the finite pointset method (FPM). A splitting technique is used to decouple the velocity–pressure computation from temperature and evolution equations. An inverse method aiming at determining chemical, thermal and rheological properties associated to the foam expansion model have been proposed. The identification procedure coupling the experimental results and the FPM simulations lead to a set of optimal parameters enabling accurate foaming simulations. The validation of the used model and the identified parameters has been achieved through the comparison between experimental and numerical short shot foams results for the foaming process in a square panel cavity with different thicknesses. An industrial foaming case consisting in an automotive underlay carpet has been simulated using the proposed model giving very similar results to those obtained experimentally by short shots method.

Acknowledgments The financial support of the European Union and the Champagne-Ardenne Region is gratefully acknowledged. This work was also supported by the HPC Centre of Champagne-Ardenne ROMEO.

References

1. Epstein PS, Plesset MS (1950) On the stability of gas bubbles in liquid-gas solutions. J Chem Phys 18:1505
2. Chang DH, Hee JY (1981) Studies on structural foam processing. IV. Bubble growth during mold filling. Polym Eng Sci 21:518
3. Amon M, Denson CD (1984) A study of the dynamics of foam growth: Analysis of the growth of closely spaced spherical bubbles. Polym Eng Sci 24:1026
4. Amon M, Denson CD (1986) A study of the dynamics of foam growth: Simplified analysis and experimental results for bulk density in structural foam molding. Polym Eng Sci 26:255

5. Arefmanesh A, Advani SG, Michaelides EE (1990) A numerical study of bubble growth during low pressure structural foam molding process. Polym Eng Sci 30:1330
6. Arefmanesh A, Advani SG (1995) Nonisothermal bubble growth in polymeric foams. Polym Eng Sci 35:252
7. Gregory AC (1972) Polyurethane foam process development. A systems engineering approach. J Appl Polym Sci 16:1387
8. Yokono H, Tsuzuku S, Hira Y, Gotoh M, Miyano Y (1985) Simulation of foaming process of polyurethane integral skin foams. Polym Eng Sci 25:959
9. Rojas AJ, Marciano JH, Williams RJ (1982) Rigid polyurethane foams: A model of the foaming process. Polym Eng Sci 25:840
10. Lee WH, Lee SW, Kang TJ, Chung K, Youn JR (2002) Processing of polyurethane/polystyrene hybrid foam and numerical simulation. Fiber Polym 3:159
11. Baser SA, Khakhar DV (1994) Modeling of the Dynamics of Water and R-11 blown polyurethane foam formation. Polym Eng Sci 34: 642
12. Bikard J, Bruchon J, Coupez T, Vergnes B (2005) Numerical prediction of the foam structure of polymeric materials by direct 3D simulation of their expansion by chemical reaction based on a multidomain method. J Mater Sci 40:5875
13. Bikard J, Bruchon J, Coupez T, Silva L (2007) Numerical simulation of 3D polyurethane expansion during manufacturing process. Colloids Surf A 309:49
14. Bouayad R, Bikard J, Agassant JF (2009) Compressible flow in a plate/plate rheometer: application to the experimental determination of reactive expansion's models parameters for polyurethane foam. Int J Mater Form 2:243
15. Baser SA, Khakhar DV (1994) Modeling of the dynamics of R-11 blown polyurethane foam formation. Polym Eng Sci 34:632
16. Lefebvre L, Keunings R (1993) Published. In: Cross M, Pittman JFT, Wood RD (eds) Mathematical modeling for materials processing. Clarendon, Oxford, p 399
17. Lefebvre L, Keunings R (1995) Finite element modelling of the flow of chemically reactive polymeric liquids. Int J Numer Meth Fl 20:319
18. Dimier F, Sbirrazzuoli N, Vergnes B, Vincent M (2004) Curing kinetics and chemorheological analysis of polyurethane formation. Polym Eng Sci 44:518
19. Piloyan GO, Ryabchikov ID, Novikora OS (1966) Determination of Activation Energies of Chemical Reactions by Differential Thermal Analysis. Nature 212:1229
20. Geier S, Winkler C, Piesche M (2009) Numerical Simulation of Mold Filling Processes with Polyurethane Foams. Chem Eng Technol 32:1438
21. Lipshitz SD, Macosko CW (1977) Kinetics and energetics of a fast polyurethane cure. J Appl Polym Sci 21:2029
22. Kuhnert J (1999) General smoothed particle hydrodynamics. PhD Thesis, University of Kaiserslautern, Germany
23. Sherman P (1962) The viscosity of emulsions. Rheol Acta 2:74
24. Serrano D, Peyrelasse J, Boned C, Harran D, Monge P (1990) Application of the percolation model to gelation of an epoxy resin. J Appl Polym Sci 39:679
25. Lucy LB (1977) A numerical approach to the testing of the fission hypothesis. Astron J 83:1013
26. Li S, Liu WK (2007) Meshfree particle methods. Springer, Berlin
27. Randles PW, Libersky LD (1996) Smoothed Particle Hydrodynamics: Some recent improvements and applications. Comput Methods Appl Mech Eng 139:375
28. Belytschko T, Lu YY, Gu L (1994) Element-free Galerkin methods. Int J Numer Methods Eng 37:229
29. Chen JS, Pan C, Wu CT, Liu WK (1996) Reproducing Kernel Particle Methods for large deformation analysis of non-linear structures. Comput Methods Appl Mech Eng 139:195
30. Lancaster P, Salkauskas K (1981) Surfaces generated by moving least squares methods. Math Comput 37:141
31. Oñate E, Idelsohn S, Zienkiewicz OC, Taylor LR, Sacco C (1996) A stabilized finite point method for analysis of fluid mechanics problems. Comput Methods Appl Mech Eng 139:315
32. Moeller A, Kuhnert J (2007) Simulation of the glass flow inside a floating process. Verre 13:28
33. Uhlmann E, Gerstenberger R, Kuhnert J (2013) Cutting Simulation with the Meshfree Finite Pointset Method. Procedia CIRP 8:391
34. Trameçon A, Kuhnert J, Mouchette L, Perrin M (2011) New Trends in Accurate Simulations for the Verification of Safety Margins in the Nuclear Power Plant Industry: Application of Virtual Performance Solution™ for the Response of Immersed Structures Subjected to Earthquakes. ASME Proc 4:409
35. Chorin AJ (1968) Numerical solution of the Navier-Stokes equations. Math Comput 22:745
36. Ivankovic M, Incarnato L, Kenny JM, Nicolais L (2003) Curing kinetics and chemorheology of epoxy/anhydride system. J Appl Polym Sci 90:3012
37. Deb K, Pratap A, Agarwal S, Meyarivan T (2002) A fast and elitist multiobjective genetic algorithm: NSGA-II. IEEE Trans Evol Comput 6:182